

Aging Dynamics in Polymer Powder Bed Fusion Systems: The Case of Selective Laser Sintering

Bruno Alexandre de Sousa Alves , Dimitrios Kontziampasis ,
Abdel-Hamid Soliman

PII: S2950-4317(25)00021-8
DOI: <https://doi.org/10.1016/j.amf.2025.200211>
Reference: AMF 200211



To appear in: *Additive Manufacturing Frontiers*

Received date: 14 October 2024
Revised date: 14 November 2024
Accepted date: 13 December 2024

Please cite this article as: Bruno Alexandre de Sousa Alves , Dimitrios Kontziampasis , Abdel-Hamid Soliman , Aging Dynamics in Polymer Powder Bed Fusion Systems: The Case of Selective Laser Sintering, *Additive Manufacturing Frontiers* (2025), doi: <https://doi.org/10.1016/j.amf.2025.200211>

This is a PDF file of an article that has undergone enhancements after acceptance, such as the addition of a cover page and metadata, and formatting for readability, but it is not yet the definitive version of record. This version will undergo additional copyediting, typesetting and review before it is published in its final form, but we are providing this version to give early visibility of the article. Please note that, during the production process, errors may be discovered which could affect the content, and all legal disclaimers that apply to the journal pertain.

© 2025 Published by Elsevier Ltd on behalf of Chinese Mechanical Engineering Society (CMES).
This is an open access article under the CC BY-NC-ND license
(<http://creativecommons.org/licenses/by-nc-nd/4.0/>)

Highlights

- Characterization of Polyamide 12 powder degradation in Selective Laser Sintering
- Microscopic images and data from aged powder dictate minor differences induced by process
- Thermal stress influences Polyamide 12 Powder Aging
- Increased material shrinkage by 0.98% is detected after six printing iterations

Journal Pre-proof

Aging Dynamics in Polymer Powder Bed Fusion Systems: The Case of Selective Laser Sintering

Bruno Alexandre de Sousa Alves ^{a, b}, Dimitrios Kontziampasis ^{c, d, e *}, Abdel-Hamid Soliman ^{a, *}

^a School of Digital, Technology, Innovation and Business, Staffordshire University, Stoke-on-Trent, Staffordshire, ST4 2DE, UK

^b Ford-Werke GmbH Henry-Ford-Straße 1, 50735 Köln, Germany

^c School of Science and Engineering, University of Dundee, Scotland, Dundee, DD1 4HN, UK

^d Dundee International Institute of Central South University, Central South University, Changsha, 410013, China

^e School of Mechanical Engineering, Faculty of Engineering and Physical Sciences, University of Leeds, Leeds, LS2 9JT, UK

*Corresponding authors

E-mail: a.soliman@staffs.ac.uk(D. Kontziampasis), d.kontziampasis@leeds.ac.uk(A. Soliman)

ORCID: Bruno Alves: 0000-0002-2716-5329, Dimitrios Kontziampasis: 0000-0002-6787-8892, Abdel-Hamid Soliman: 0000-0001-7382-1107

Abstract

Additive manufacturing (AM) is an advanced production method for layer-by-layer fabrication, offering a paradigm shift in manufacturing. However, the sustainability of AM processes is poor, since suppliers recommend reusing 50%-70% of reprocessed powder, contributing to a significant increase in material disposal.

To explore the possibility of fully reusing the polymeric material, we conduct a comprehensive characterisation of the powder particulates, in combination with analysis of the final prints. Utilizing optical and scanning electron microscopes, we statistically evaluate the size, morphology, and shape of the particles. Furthermore, tensile strength and deformation of printed bars is evaluated, showcasing the impact of aging on the print properties. The findings reveal that consecutive reuse of used powder significantly influences dimensional accuracy of the printed parts. We detect a 30.63% relative value of shrinkage after six printing iterations, which corresponds to an absolute shrinkage increase by 0.98%. This is significant considering the standard shrinkage for the material used is already 3.2%. Additionally, parts that are printed with reused material exhibit a small increase in elongation at yield, as well as an unexpected rise in tensile strength. Significant agglomeration of small particles is observed in the aged powder, since there are particles of less than 10 μm , which are not found in the virgin powder. These results contribute to a better understanding of the issues related to the reusing of aged material, and offer invaluable insights for mitigating the environmental impact that is associated with material disposal in AM.

Keywords: Additive manufacturing; 3D printing; Selective laser sintering; Polymers; Sustainability; Recycling

1. Introduction

Additive manufacturing (AM) is a general term used to define a manufacturing process that employs layer-by-layer building of parts. Other common names of AM are 3D printing and rapid prototyping. One category of techniques of AM is referred to as Powder Bed Fusion, where Selective Laser Sintering (SLS) process belongs. SLS currently stands out as one of the most established and widely employed additive manufacturing techniques in industry [1]. It employs the use of polymeric particulates, that range from semi-crystalline, as for example polyamide 12 (poly(dodecano-12-lactam), **PA12**, Nylon12, Nylon), to amorphous, as for example thermoplastic polyurethanes (TPU). This powder-based process sinters objects layer by layer using one or numerous lasers, and as such it offers the possibility to print extremely complex parts without the need of support creation structures. The surrounding powder acts as a support of the printed part. Typically, for applications where high mechanical strength and minimal warpage is required, PA12 is preferred in industry [1].

Regardless of all the aforementioned advantages of utilizing the SLS process with PA12, a major consideration arises. The limited volume ratio of particles that effectively undergo sintering. Typically, only a fraction (5%-15%) of the total amount of particles within the build chamber become part of the printed object. This is commonly referred to as the packing density, which quantifies the ratio of volume that is occupied by the sintered object's material, to the total volume within the build chamber. In more detail, packing density allows for the measurement and the evaluation of the efficiency of particle utilization, i.e. for the amount of polymeric particulates that are printed throughout the SLS process. The remaining 85%-95% of the surrounding particles undergo numerous physical and chemical degradations throughout the build process, i.e. pre-heating, sintering, cooling, and post-treatment stages [2]. A portion of the particles are reused in subsequent builds, typically mixed with 50-70% virgin powder, while all the remaining materials is disposed. Evidently, a significant opportunity for recycling and further utilization of this material arises [2]. Scientific literature consistently indicates that these affected particulates exhibit non beneficial surface morphologies, partial restructuring through larger and more complex molecular chains, reduced particulate flowability, as well as altered mechanical and thermal properties [1], [2], [3]. These findings, even though on most cases sporadic, provide a glimpse towards the weight and the importance of directly reintegrating aged polymeric particulates into the SLS process, showcasing the complexity of the named challenge, and clearly pointing out the need for a systematic study to fully understand the totality of the effect of the process on the polymeric particulates.

The current normal situation in industry is to dispose the material, not only carries a significant financial hurdle (~118 €/kg in 2023 [4]), but also contributes to environmental pollution[5]. Therefore, it is imperative that one studies the potential of maximizing the reuse of the total amount of the material. In parallel, it is becoming obvious that we need to understand the way on how AM will produce no waste material in the end of the final cycle, i.e. investigate how AM will become a truly sustainable manufacturing method [1]. When working with particulates, powder flowability is an important property that one needs to consider, since it denotes the material's ability to flow freely and consistently, pinpointing it as a critical factor in facilitating the powder processing of the powder bed fusion process, since in the apparatus (recoater) there is a carry and deposition of particulates in layers, flowability is essential for optimal performance. Higher sphericity enhances flowability, while deviations such as a potato-shaped design decrease it. The least favourable scenario would involve the flowability of irregular particles with rough edges, whereas one would measure the poorest flowability [6].

There are numerous papers in literature that extensively explore the use of aged powder across various processes. Yang et al. [1] show the process control of selective laser sintering with interlayer heating, preprocessing, and material mixings. This process not only preserves but also enhances the mechanical

properties of 3D printed parts made from recycled PA12 powder, even with heavily aged powder that are typically challenging to reuse due to thermal degradation. By increasing tensile strength by approximately 18% and elongation at break by around 55% compared to standard methods, their approach offers a path towards more sustainable 3D printing practices. It also provides a boost towards research that is aligning with goals for improved material efficiency and durability in additive manufacturing. A different study [7] proposes the reuse of aged, degraded PA12 from SLS, where they transform the particulate material into filaments, in order for them to be used for printing with a different AM process, called fused deposition modelling (FDM). Wang et al. [8] demonstrate a recycling method by mixing the powder with milled carbon fibre/recycled PA12 composite filaments in order to be reused. Paolucci et al. [9] show the impact of elevated temperatures on the isothermal crystallization kinetics of PA12. Ford Motor Company also patented an apparatus for treatment of residual thermoplastic powder, that converts the powder into pellets, so it can be reused using in high injection moulding machine [10]. The ageing mechanisms of thermal and coalescence behaviour are studied in Refs. [2][3] and how this affects crystallinity, microstructure, and mechanical properties of the particulates, in an effort to characterize the aging process. Others Refs. [11], [12], [13] verified the decreased flowability of aged PA12 powders compared to that of virgin, providing a means to measure powder degradation rates. Wudy et al. [14], [15] investigated the influence of processing time and temperature on the aging effects of PA12 in SLS. Specifically, they studied molecular changes and thermal property changes of PA12 part cake materials and examined the ageing behaviour specific in SLS, including bulk characteristics and part properties, i.e. porosity and surface roughness. Goodridge et al. [16] and Wudy et al. [17], studied the effect of powder reuse on mechanical properties, where they noted changes in tensile strength and elongation at break point in the parts that were built from aged PA12 powders. One key finding from this study is that partially degraded powder often needs to be mixed with fresh powder, in order to maintain the quality and consistency of laser-sintered parts. This "refreshing" approach mitigates the effects of thermal degradation, however, inconsistencies in the aging levels of the recycled powder can still lead to a wide variability in part properties. Initiating from physical and chemical degradation, the aging mechanism of PA 12 particulates in laser sintering involves a complex interaction of numerous processes. Physical degradation, which is considered reversible, primarily manifests as alterations in molecule order and concentration, particle post-crystallization, and agglomeration[12], whereas fine particles adhere to each other to form larger aggregates or clusters. On the contrary, chemical degradation, marked by irreversibility, takes precedence in dictating the aging process, inducing transformative changes in polymer structures. This chemical degradation involves phenomena as for example chain scission, where covalent bonds within the polymer structure of PA are ruptured resulting in the formation of smaller chains, and cross-linking, which can be catalysed by oxidation. When the polymeric particles are exposed to elevated temperatures, i.e. 180°C for the case of PA12, the polymer itself undergoes oxidative degradation that induces changes in strength and rigidity. Chemical degradation also involves post-condensation, with both thermal oxidation and post-condensation emerging as the dominant aging mechanisms identified in available research for the chemical degradation of PA12 during SLS [3], [17]. Post-condensation process includes phenomena as for example the elongation of polymer molecular chains through the combination of free radicals at elevated temperatures, which consequently alters the molecular weight, flowability, and viscosity. Additionally, chemical degradation also includes hydrolysis, in which water molecules break the bonds between monomers in a polymer chain [1].

While there is ample information available in literature on the aging mechanisms of PA 12, the consequences of utilizing aged polymeric particulates, as well the effect of aging on physical and chemical properties of both the particles and the prints is not systematically examined, analyzed, and documented. It is imperative to use these in order to decode and comprehend the necessary adaptations in the 3D design and the machine parameters in order to optimise any use of aged polymeric particulates in powder bed fusion AM. This paper initiates a systematic study that aims to fully comprehend and decode how the use of aged PA12 polymer particulates in SLS affects the finalised print. The ultimate goal of this paper is not to

reproduce parts with identical quality, but to understand the direct effect of the use of aged particulates. This is achieved by analysis and characterization of both the particulates themselves, as well as the finalized printed parts. It is the first study in literature to incorporate the reuse of particulates for 6 consecutive cycles. This allows for evaluation of the effect of the AM process itself on particles and prints produced, via directly comparing them with the equivalent when unused particulates are employed. Particle size and its distribution are characterised using microscopy and analysing statistically the size and shape of particulate. Subsequently, mechanical properties of the prints are analysed with the use of stress-strain diagrams, also noting down the effect of aging of particles on size for all the produced prints.

2. Materials and Methods

2.1 Details on experimental apparatus, process, and materials

For the 3D printing tests, a standard machine Fuse 1+ 30 W from Formlabs was used [18-20], which is equipped with a 30 W fibre laser that print speeds of up to 12.5 meters per second. The spot size of the laser is 200 micrometres, and it includes a galvanometer driven system. The material of choice for these tests was PA12 powder from Formlabs, product number: PD-FS-P12G-01, Batch: 952863. This PA12 material is a favourite material of choice in a plethora of industries, for both functional prototyping, as well as end-use production of complex assemblies and durable parts with high environmental stability [21].

For optical analysis a Keyence VHX-5000 microscope was used, equipped with digital imaging technology to capture high-resolution images of the acquired particle samples (see Table 1). Scanning electron microscopy was done using a Zeiss Gemini series for imaging and analysis.

Table 1. Particle samples.

	Series particles			Total
	A	B	C	
Batch 1	2563	1234	681	4478
Batch 2	1626	1555	903	4084
Batch 3	936	1009	569	2514
Batch 4	1462	1176	1340	3978
Batch 5	2654	1500	811	4965
Batch 6	1494	1087	813	4995

The mechanical tensile tests were performed using the stress-strain apparatus Galdabini Quasar 50 kN, operating at 23°C with 50% relative humidity. The tests were conducted at a speed of 50 mm/min.

As shown schematically in Fig. 1, there are several key components on the Selective Laser Sintering machine that need to be mentioned, such as the build platform, powder delivery system, heating system, and the optical system. On the build platform, the size determines the maximum part dimension that could be printed, while the powder delivery system, including the recoater, ensures even distribution of powdered material across the platform. The heating system preheats the powder bed within the chamber to an optimal temperature and during the entire selective sintering process the surround part powder is kept just below its melting temperature [18], to enhance adhesion between successive layers and facilitating uniform sintering. The optical system that guides the laser beam precisely to sinter the material according to data, includes

mirrors and lenses and is one of the crucial components in the method, requiring regular cleaning and maintenance to ensure it remains in optimal condition. Initiating the process, the laser melts the powder locally on the respective layer, sintering the part contour, after printed the first layer, the build platform is moved downwards, and a new powder layer is laid off using the recoater. After successive layers the complete sintered part is produced [18].

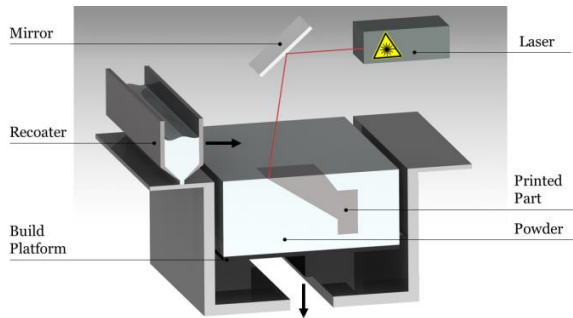


Fig. 1. Graphic representation of a Selective Laser Sintering machine, showing all key components.

Typically, the quality of the starting material varies significantly on each print, due to the different percentages of new and aged powder used, as well as the packing density used in previous prints. This renders it extremely challenging to predict and know precisely how many successive builds each PA12 powder particle was involved previously. To avoid this scenario, it was decided to follow the following protocol. Every series of experiments starts from 100% virgin material. In each of this series there is no new unused virgin material that is added. Every time there is a print cycle, we extract material and we use it for analysis with microscopy. Each series consists of 6 cycles of printing, meaning that the powder starts as virgin, and ends to be reused 5 times in the final printing cycle (see Table 2). For statistical purposes, and to showcase the same trend, there are 3 series of experiments performed, named A, B, and C. Following this approach in preparing samples, allows for clear detection of any differentiation in the properties of the particulates and prints.

Table 2. Description of the powder state in each batch.

Machine batch description	Powder state
PA12 - 1	100% Virgin new powder
PA12 - 2	Aged powder reused 100% - 1 time
PA12 - 3	Aged powder reused 100% - 2 times
PA12 - 4	Aged powder reused 100% - 3 times
PA12 - 5	Aged powder reused 100% - 4 times
PA12 - 6	Aged powder reused 100% - 5 times

2.2 Printing process

The experiment involving the printing of tensile bars shown in Fig. 2(b). The tensile specimen was designed according to the ISO 527-2 standard, specifically Type A1. ISO 527-2 is a widely recognized international standard that outlines the testing methods for determining the tensile properties of plastic materials, including specimen dimensions, preparation, and testing conditions. The tensile bars were

positioned inside the build platform and repeated consecutively **6** times, referred to as batches PA12-1, to PA12-6 respectively. Within each batch, **9** tensile bars were strategically positioned in the build platform, as illustrated in Fig. 2(a). To ensure robust statistical outcomes, all tests were repeated three times, labelled as **Series A**, **Series B** and **Series C**, and created results averages. Within each series, the tensile bar was printed 9x6 batches, comprises a total of **54** tensile bars in each Serie, contributing to a cumulative total of **162** tensile bars printed for the entire research.

In order to detect the thermal ageing of PA12 powder, the machine was initially fed with 100% virgin powder - Table 4 (PA12-0) and reused 100% the powder for the successive builds **without** refreshing it.

The 3D printing machine Fuse1+ was started following exactly the numerations and position of the tensile bars showed in the Fig. 2(a). The printing direction is a well-documented factor that is affecting the mechanical properties of SLS specimens and is influencing part strength and consistency [20]. These properties can vary depending on the print orientation due to differences in how the layers bond and the alignment of polymer chains. It should be noted that the tensile bar specimens were printed utilizing 6 kg of virgin powder with a packing density of 2%. Each printing process required a total of 14 hours and 21 min for completion, and the build box was allowed to cool for 14 h before further handling. Each batch box was printed in 2727 layers.

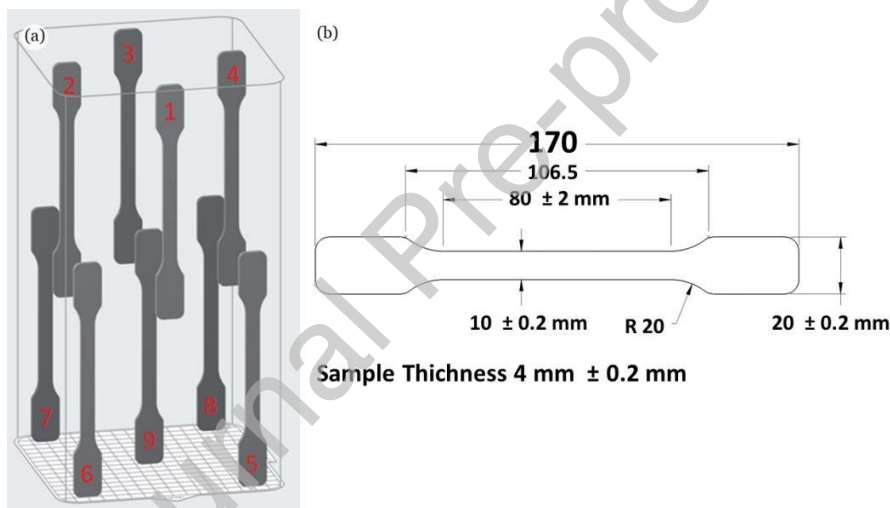


Fig. 2. (a) Tensile specimens ISO 527-2 Type A1 position inside the SLS machine; (b) Dimensions for specimen ISO 527-2 Type A1 Standard [19].

Following printing and cooling down the parts, the operator manually used the standard post-processing cleaning station (Fuse Sift from Formlabs) to remove and clean the tensile bars, collecting 100 g of the powder for further analysis. The remaining powder was filtered using a sieve with a mesh size of 150 μ m to remove any small chunks or debris and ensure the powder remained clean [21].

After filtering the powder, the SLS machine was loaded with the powder material and restarted the successive building process, following the printing sequence shown in Table 2.

3. Results and Discussion

3.1. Effect of aging on print dimensions

The experiments conducted aim at the dimensional verification of the printed tensile specimens, with standard nominal values for thickness (4 mm) and width (10 mm) and a specified tolerance of ± 0.2 mm. A total of 162 tensile bars are successfully printed, which corresponds to 54 tensile bars per series of experiments.

All tensile specimens (Fig. 3) from each of the three series (A, B and C) are measured, and average values across the series are calculated and further analysed, (see S1, S2.)

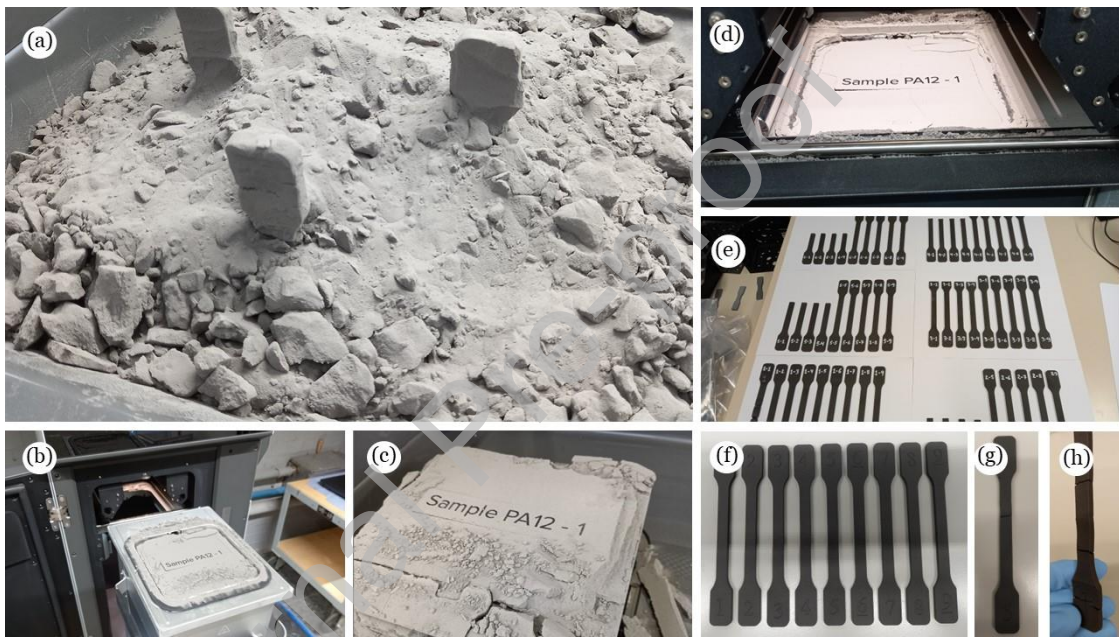


Fig. 3. (a) Tensile specimens in cleaning process; (b,c,d) Build box with powder and printed parts; (e,f) Printed tensile specimens; (g,h) Printed Tensile Specimen with defects.

It should be noted that from the 162 tensile bar samples that were printed, only 1 was out of tolerance. However, based on the dimensional results, a decrease is observed in both the width and the thickness of the tensile bars as the powder degrades. This can be seen in Fig. 4. The parts gradually become smaller as one continues to reuse powder without refreshing it with new powder. Conversely, it is also observed that using 100% virgin powder results in a positive deviation, meaning that the parts in the first batch are bigger than the nominal value. These results are a clear demonstration that the quality and degradation of the powder influences directly the dimensions of the printed parts. To quantify, this analysis documents an increase of the material shrinkage factor by 0.98% after 6 cycles. For reference, the standard shrinkage factor for the specific PA12 used in the study is 3.2%. Via direct comparison of these two, it is evident that the observed increase in shrinkage factor of 0.98% is indeed significant, and as this influence directly the final dimensions of the part, it is 30% more in terms of the shrinkage factor.

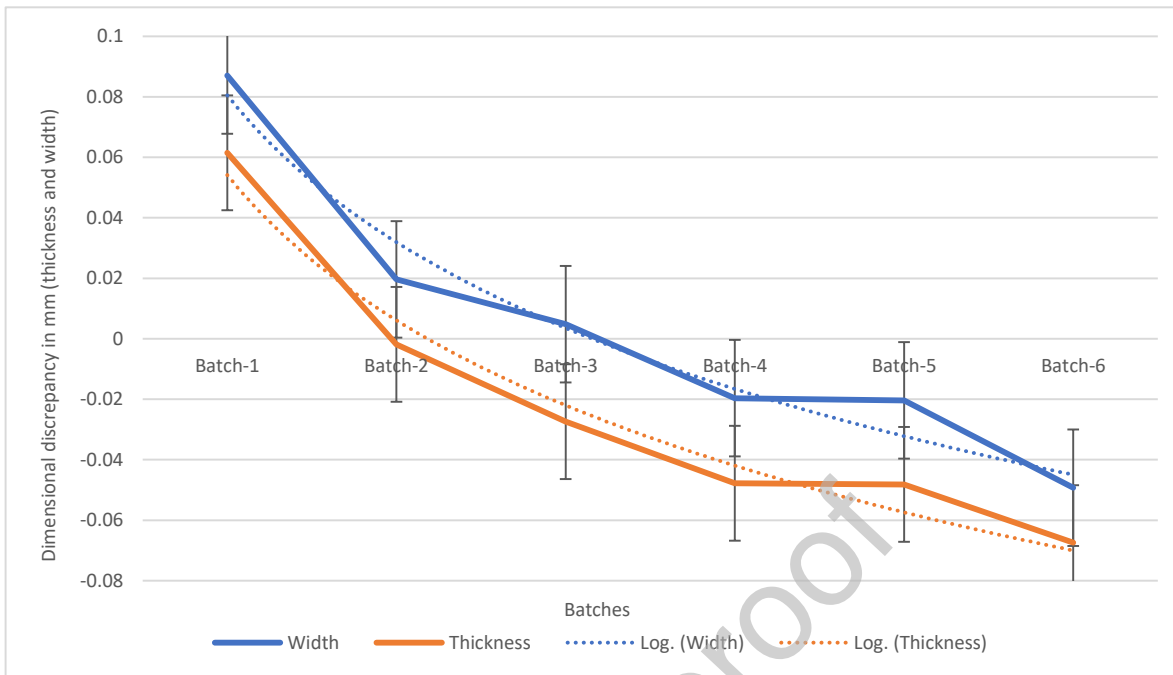


Fig. 4. Average tensile bar thickness and width discrepancy to nominal values, using successively aged powder 6 consecutive times.

Given the complexity of selectively laser sintering, it is reasonable to assume that multiple factors can influence printing quality, and lead to the observed increase of shrinkage of the print. When PA12 particles undergo degradation, potential factors may include changes in particle size distribution, variations in thermal properties (i.e. melting point, material density), as well as changes in chemical composition (Fig. 5). These changes influence how the material solidifies and consolidates during the AM process, ultimately impacting the overall shrinkage behaviour.

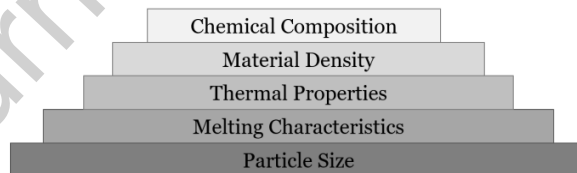


Fig. 5. Factors that may have Influence in the Increase Shrinkage factor.

3.2 Effect of aging on PA12 particulate size and shape

This set of experiments involves the collection of PA12 particle samples from every batch after printing the tensile bars as explained in Section 2, and the subsequent analysis of the particles with optical microscopy and SEM. The goal is to determine whether the increase in shrinkage can be attributed to variations in particle size distribution, morphology, and composition. With microscopic analysis we are able to detect variations in powder diameter, considering the “potato-like” shape of the PA particles.

The results indicate that the particle size distribution has undergone changes, but these cannot be deemed as significant. As shown in Figs. 6-13, the majority of particles fall within the range of 50 μm to 70

μm . Upon comparing all the three series from the acquired particle samples, there was no consistent and clear alteration in distribution, on either side, showcasing the consistency of the particulate size throughout the experiments. This clearly proves that size of the PA12 particulates is not affected by aging in the examined process. However, it was observed that there is agglomeration of small particles, especially those less than $10\ \mu\text{m}$ in the aged powder, a phenomenon that is not present in the virgin powder.

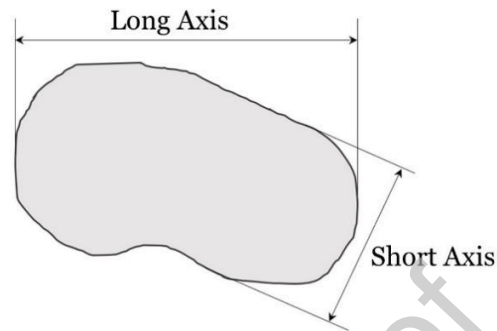


Fig. 6. Schematic representation of a typical PA12 particle cross section.

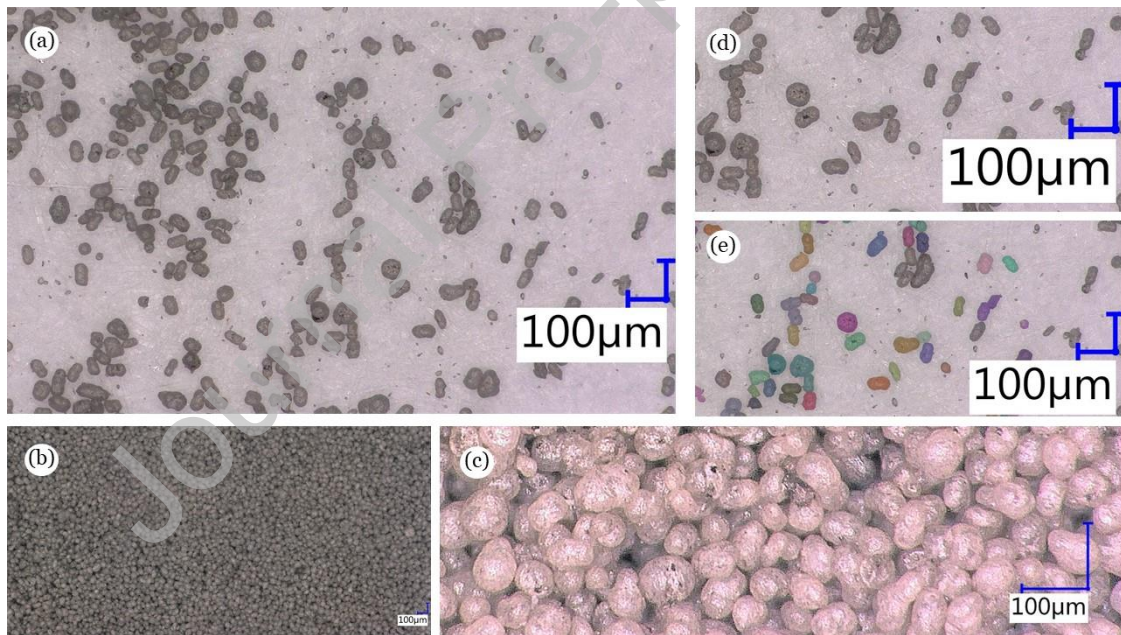


Fig. 7. (a-e) Optical microscope images showing characteristic size and shape of particles from Batch PA12 – 1 (Series A).

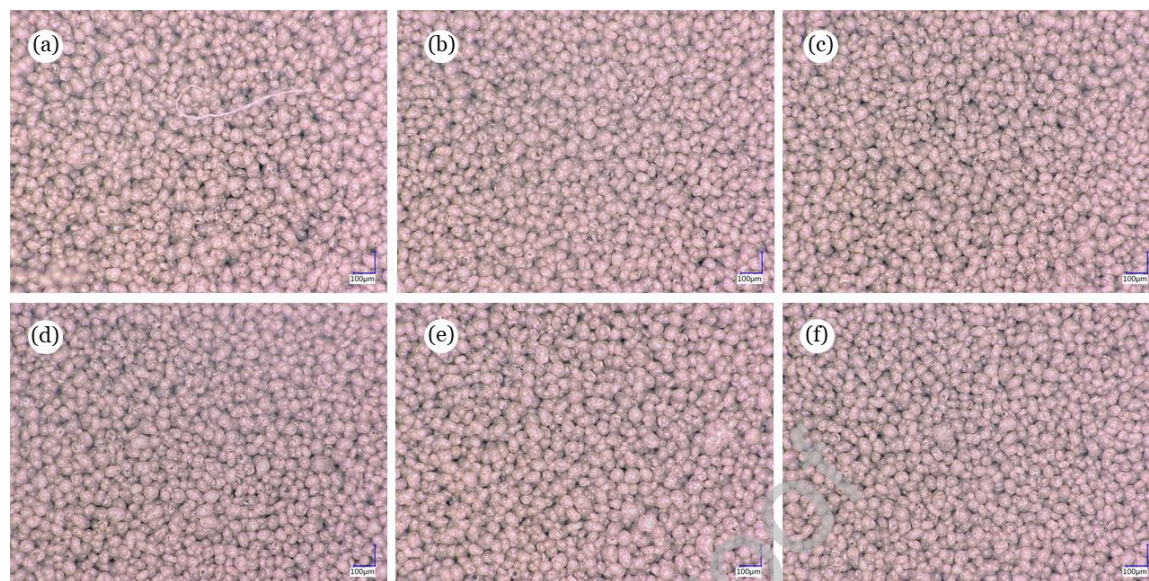


Fig. 8. Optical microscope images of particles from Series A: (a) Batch PA12 – 1; (b) Batch PA12 – 2; (c) Batch PA12 – 3; (d) Batch PA12 – 4; (e) Batch PA12 – 5; (f) Batch PA12 – 6.

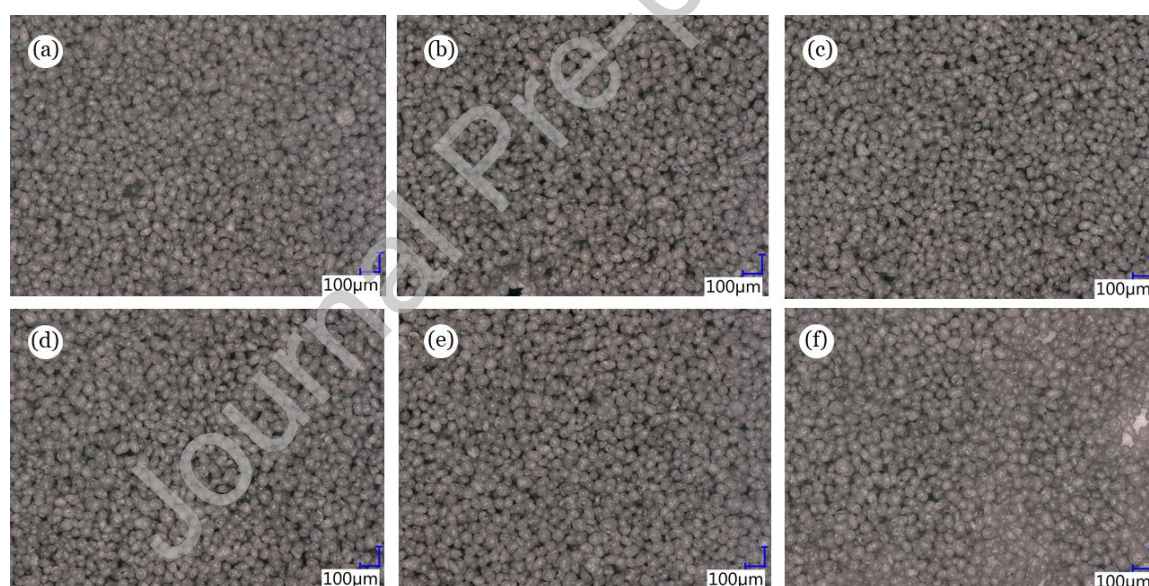


Fig. 9. Optical microscope images of particles from Series A: (a) Batch PA12 – 1; (b) Batch PA12 – 2; (c) Batch PA12 – 3; (d) Batch PA12 – 4; (e) Batch PA12 – 5; (f) Batch PA12 – 6.

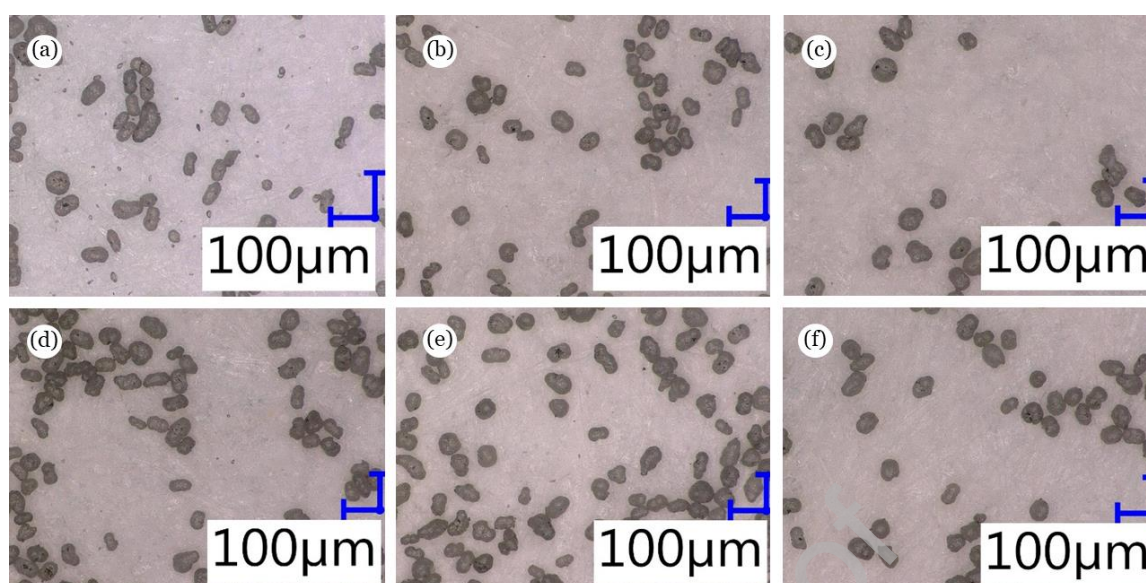


Fig. 10. Optical microscope images of particles from Series A: (a) Batch PA12 – 1; (b) Batch PA12 – 2; (c) Batch PA12 – 3; (d) Batch PA12 – 4; (e) Batch PA12 – 5; (f) Batch PA12 – 6.

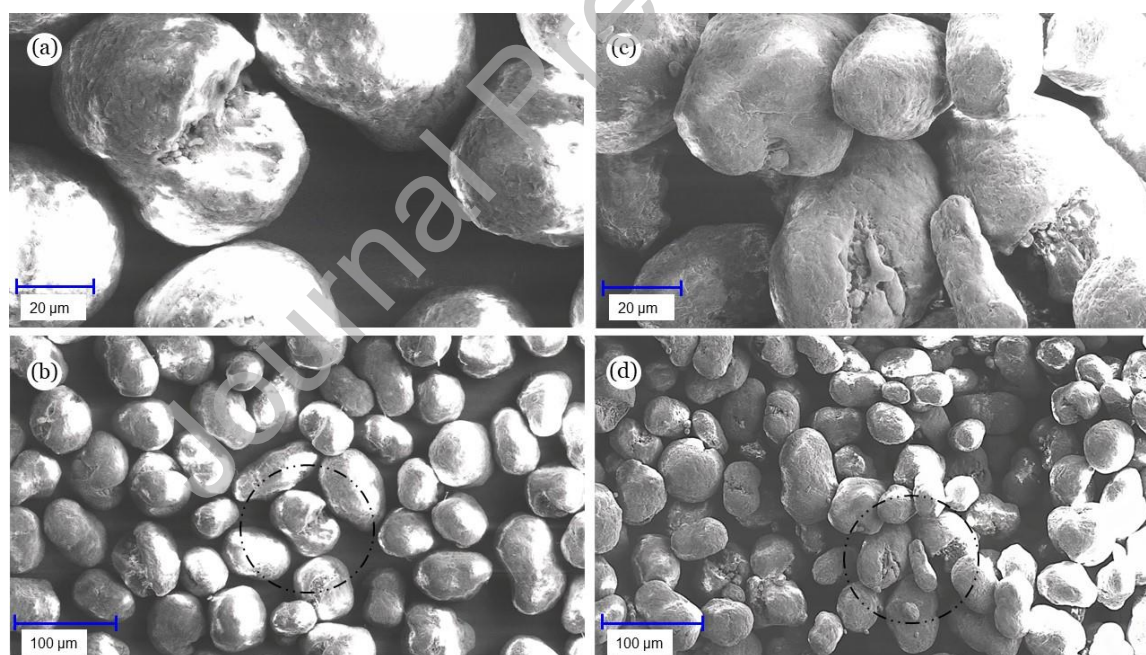


Fig. 11. (a,b): Scanning electron microscope (SEM) images of virgin PA12 particulates; (c,d): Scanning electron microscope (SEM) image of aged PA12 particulates.



Fig. 12. Scanning electron microscope (SEM) image of SLS Aged PA12 showing details of the particles on the surface, as well as their different sizes and shapes.

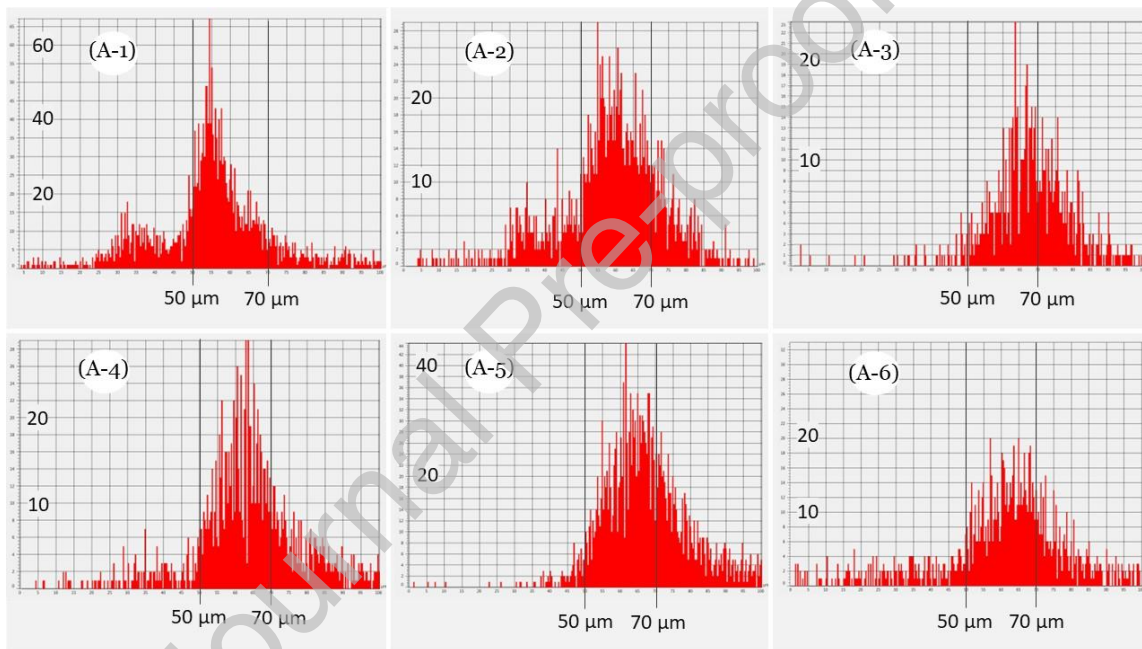


Fig. 13. Particle size distribution (Series A, for Batch 1 to 6) (X-axes represent the particle size, Y-axes represent the number of particles within each size range).

To further comprehend this agglomeration process, SEM images were taken and examined, revealing the presence of very small particles mixed with the potato-shaped powder particles. In this analysis, an average ratio of 1.5 was detected (long axis divided by short axis). A ratio of 1 represents a spherical particle, which is advantageous for its flowability, packing efficiency, and uniformity in the powder bed, leading to improved printing results. However, the findings indicate that the particles exhibit an average ratio of approximately 1.5, as can be seen in Fig. 14. This deviation from perfect sphericity suggests that the particles are elongated or in some cases also irregular. It's also important to note that in virgin powder, particles with defects were also observed, appearing broken and with deep recesses. We did not assess whether these issues stem from the powder supplier production method, but they undoubtedly influence the powder flowability. Further studies are required implementing the use of different suppliers to generalize the above findings.

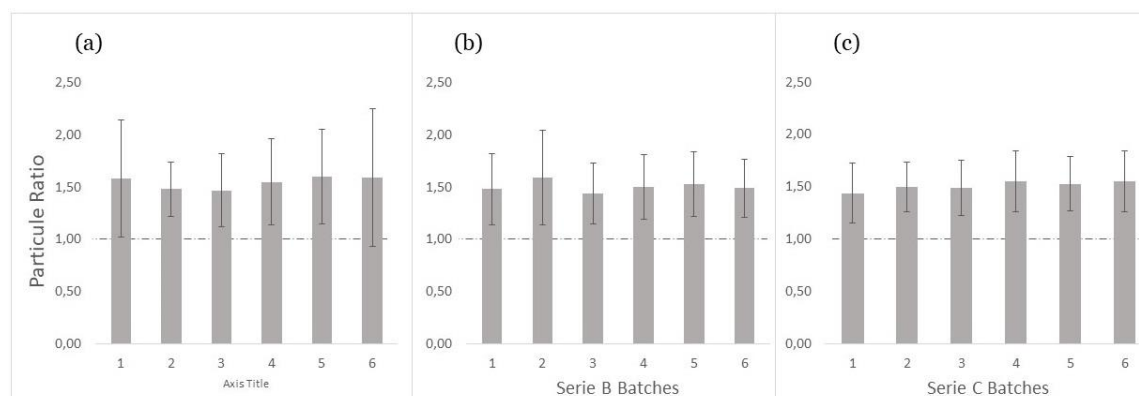


Fig. 14. Particles shape ratio: A ratio of 1 (long axis divided by short axis) shows a spherical particle, however, this analysis reveals the prevalence of elongated, potato-shaped particles, with an average ratio of ~1.5.

The behaviour of PA12 powder particle size during degradation was analyzed, and based on the results (Figs. 15), it appears that it depends on various factors. There is no global rule that applies to all cases though. However, in some instances, as for example batch 4 and batch 6, the degradation of particles led to a decrease in particle size. The degradation processes, such as thermal or mechanical breakdown, can result in the fragmentation of particles into smaller sizes. It was also observed that there is an increase in particle size for batches 2, 3, and 5, which shows that powder may agglomerate, and this leads to the presence of larger particle clusters. Particle coarsening could also be present, as ageing can cause individual particles to coarsen, resulting in an overall increase in particle size. Another cause could be environmental effects, as for example moisture absorption, as aged powder is susceptible to more time under open conditions and may absorb moisture, which can cause particles to swell and increase in size. Despite the challenges in controlling all boundary conditions, the water content in the surrounding environment should not be disregarded in PA12 materials. Another conclusion from this analysis, is that it suggests that the packing density of 2% has a subtle effect on the average diameter of the particles and it does not appear to have an effect on the morphology of the particles themselves.

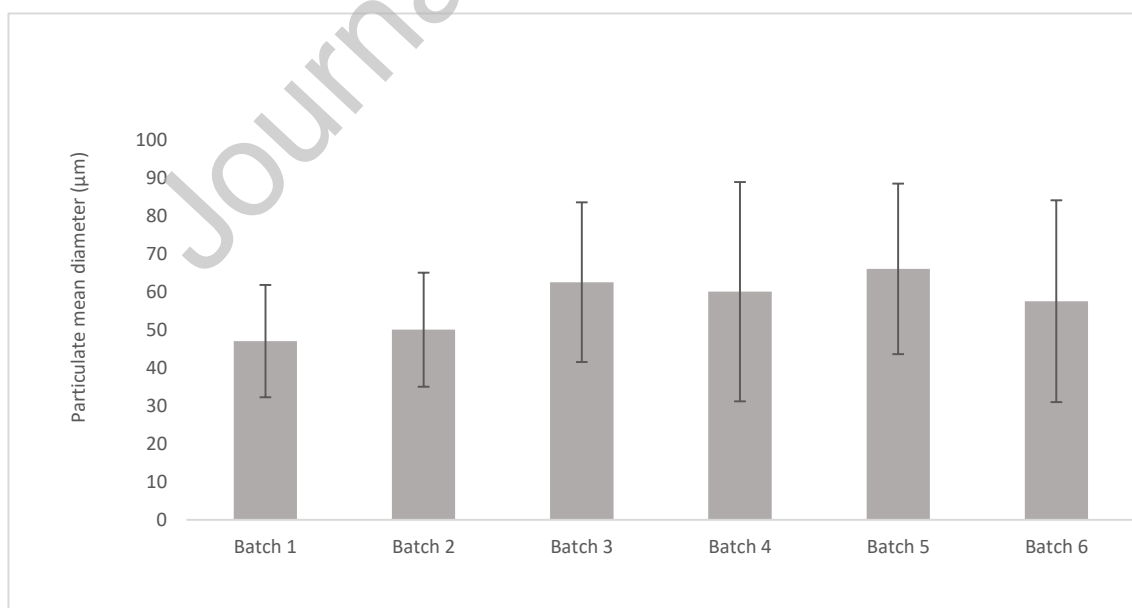


Fig. 15. PA12 particle size series A (Mean maximum and minimum from batch 1 to 6).

In conclusion, Series A showed a slight increase in particle diameter, Series B showed no conclusive change, and Series C showed a slight decrease (Table. 3). Taken into consideration the experimental error, these results suggest that there is not clear trend or a change in the diameter further research is needed to fully understand the underlying process.

Table 3. Powder particle dimensional data analysis as combined average across series A, B, C.

		Surface area (μm^2)	Short axis (μm)	Long axis (μm)	Mean diameter (μm)
Batch 1*	Average	2145	42	62	52
	Normal deviation	905	12	17	
Batch 2*	Average	1777	37	54	46
	Normal deviation	921	13	19	
Batch 3*	Average	2350	44	65	55
	Normal deviation	1038	12	20	
Batch 4*	Average	2146	41	64	46
	Normal deviation	1144	13	26	
Batch 5*	Average	2277	43	65	53
	Normal deviation	983	11	18	
Batch 6*	Average	2084	41	61	51
	Normal deviation	1012	12	19	

3.3 Effect of aging on the mechanical properties of the prints

In this Section, the strength of the tensile bars that are manufactured in each respective batch is evaluated (Fig. 16). To assess this, tensile bar testing under specific climate conditions (DIN EN ISO 291:2008-08): 23°C / 50% rel. LF is conducted. All experiments are performed at a speed of 50 mm/min and can be found in the Supplementary Material (Figs. S13- S39).

The goal is to detect variations in the tensile strength and the ductility of tensile bars that are produced using the aged powder. Understanding these differences will help machine operators to adapt the recycling ratios, and to balance new and aged powder, while maintaining quality standards. Additionally, it is imperative when using aged particles to anticipate differences in quality, to proactively introduce corrections that can mitigate potential deviations from desired standards and ensure consistency in performance, which is fundamental for repeatability and reliability across printed parts.

In Table 4, a comparison between the first batch (virgin powder) and the last batch (aged powder) reveals a slight increase in the elongation at yield %, as well as a counterintuitive increase in tensile strength. In general terms, a decline in the Young's Modulus suggest that the material can undergo more deformation before yielding or breaking, explaining this behaviour. The changes due to aging appear to promote the increase of plastic deformation and contribute to increased ductility. This directly impacts the print's capacity to revert to its original shape after deformation, leading furthermore to a lower tensile modulus. Notably, the tensile modulus of PA12 powders that are used six times, showed significant differences between the maximum and minimum, the highest difference reaching 1039 MPa. This difference can be attributed to various factors. Initially, repeated heat exposure during the printing process has the capacity to alter the powder's thermal and mechanical properties, a fact that can potentially lead to polymer chain degradation or crosslinking, which subsequently impacts stiffness. Additionally, each reuse can generate finer particles, as can be evidenced in the microscopy images, which can significantly alter the packing

density and affect bonding. Larger particles typically improve bonding, while smaller ones tend to reduce its strength [22]. The repeated heating and cooling cycles of the printing process also potentially has the ability to weaken inter-layer bonds, especially in the case where sintering is incomplete, which in turn affects the tensile modulus [22] of the print.

Table 4. Comparison of tensile bar averages across three series: first batch vs. last batch (see supplementary material).

Tensile bar No.	Batch 1 (Virgin powder)			Batch 6 (Aged powder)		
	Elongation at yield (%)	Tensile strength (MPa)	Tensile modulus (MPa)	Elongation at yield (%)	Tensile strength (MPa)	Tensile modulus (MPa)
1	2,02	25,44	1938,40	4,42	48,82	1342,57
2	4,80	49,78	2101,97	4,39	47,02	1207,03
3	4,14	52,23	2251,20	4,97	47,63	1190,50
4	4,86	49,43	2146,30	4,39	47,64	1028,13
5	2,37	27,67	1924,77	4,17	47,54	1903,97
6	2,98	41,98	2001,03	3,84	46,79	2032,07
7	4,05	48,57	1925,10	3,28	44,61	1847,90
8	4,27	48,62	2036,97	4,41	47,90	2067,17
9	4,28	49,44	1911,00	4,21	47,59	2066,13
Average	3,75	43,68	2026,30	4,23	47,28	1631,72

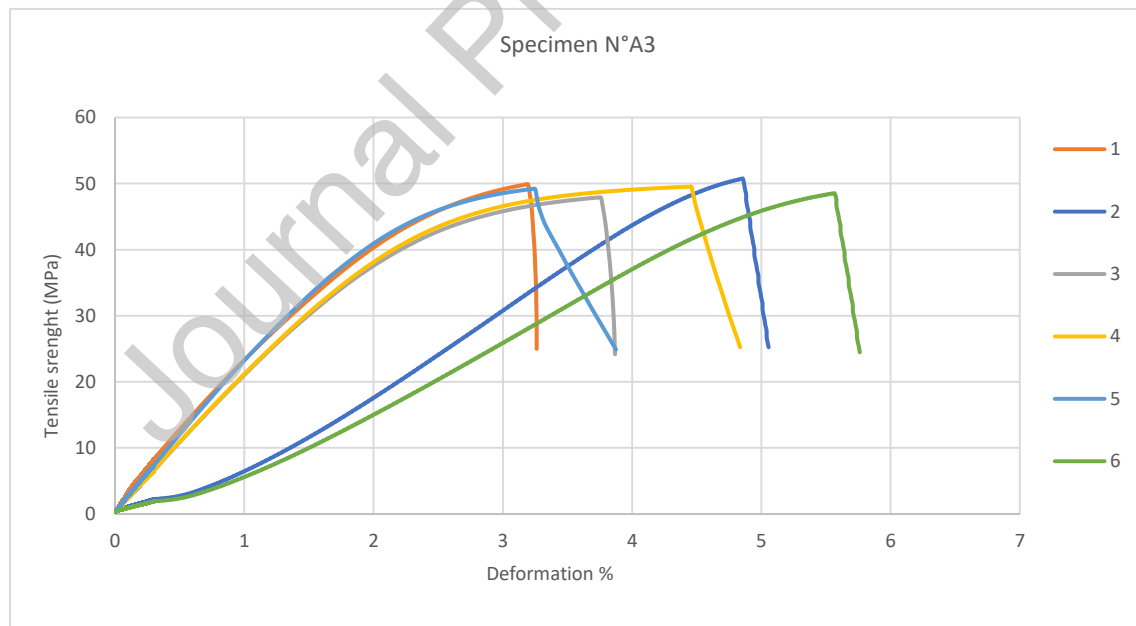


Fig. 16. Example of stress-strain diagrams that are plotted for the comparison of tensile bar number 3 across all six batches in Series A.

4. Conclusion

(1) This work evidences through characterization, analysis, and experimental results, that consecutive reuse of old powder is achievable for PBF methods, and SLS in specific. The results clearly prove that aging has a direct dimensional impact on the printed parts for SLS is used. Using only reused powder, directly results in a 30% increase of the relative shrinkage of the print, when compared to the prints produced with the use of mixed powders. Following the findings as described above in this study, one can successfully minimize the effect of aging on the produced prints.

(2) The results have a direct impact in the control of the process. They show how a machine operator can reduce dimensional errors by updating the object scale factor accordingly, before initiating any print operations, via increasing or decreasing it depending on the aged powder quality. It is important to note that this consideration applies only in the cases where aged or extremely aged powder is used. Otherwise, a standard scale factor can be employed in a case-by-case scenario. Interestingly, the decrease in thickness and width of the tensile bar does not appear to have a significant effect on its overall tensile strength and performance.

(3) Regarding the effect of aging on particle size, shape, and distribution, the packing density used to print the tensile bars of 2%, has a subtle effect on the average diameter of the particles, with a minuscule increase observed, as a result of aging. The morphology of the particles does not appear to have significant differences. However, there is notable agglomeration documented from the microscopy images. There are numerous small particles observed in the aged powder, with less than 10 μm diameters, which are not present in the virgin powder.

(4) Following the machine use protocols that are already developed in most labs, the powder is sieved to filter agglomerated particles between each build, typically with a 150 μm sieve, in order to minimize the possibility of blocking. However, smaller particles typically remain in the powder, a fact that highlights the need for the development of new steps that will remove these fine particles, either through the use of smaller sieves or other alternative methods.

Overall, this work and its findings come to provide a sound basis and to contribute to the general understanding of the aging behaviour and its effect on the properties of PA12 particles undergoing the specific conditions of laser powder bed fusion techniques. This is a necessary first step that will inform future improvements in manufacturing and design processes and will have a direct impact on improving the sustainability of the method. The final goal is to succeed into making powder bed fusion sustainable, successfully reuse all the initial powder, and aid the current global effort to soon transition to sustainable manufacturing technologies.

CRediT authorship contribution statement

Bruno Alexandre de Sousa Alves: Formal analysis, Investigation, Methodology, Validation, Writing – original draft. **Dimitrios Kontziampasis:** Conceptualization, Formal analysis, Supervision, Validation, Writing – review & editing. **Abdel-Hamid Soliman:** Conceptualization, Project administration, Supervision, Writing – review & editing.

Declaration of Competing Interest

The authors declare that they have no known competing financial interests or personal relationships that could have influenced the work reported in this paper.

Acknowledgement

The authors declare that they have no known competing financial interests or personal relationships that could have influenced the work reported in this paper.

Supplementary Materials

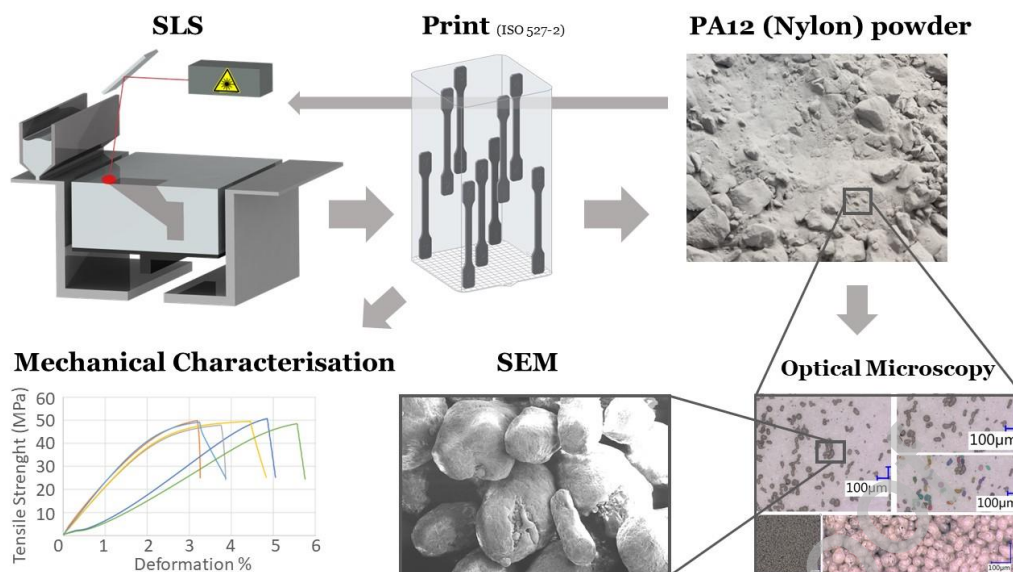
The authors confirm that the data supporting the findings of this study are available within the article.

References

1. Yang F, Jiang T, Lalier G, et al. A process control and interlayer heating approach to reuse polyamide 12 powders and create parts with improved mechanical properties in selective laser sintering. *J Manuf Process* 2020;57:828-846. doi: 10.1016/j.jmapro.2020.07.051.
2. Chen P, Tang M, Zhu W, et al. Systematical mechanism of Polyamide-12 aging and its micro-structural evolution during laser sintering. *Polym Test* 2018;67:370-379. doi: 10.1016/j.polymertesting.2018.03.035.
3. Dadbakhsh S, Verbelen L, Verkinderen O, et al. Effect of PA12 powder reuse on coalescence behaviour and microstructure of SLS parts. *Eur Polym J* 2017;92:250-262. doi: 10.1016/j.eurpolymj.2017.05.014.
4. Formlabs Nylon PA 12 SLS-Powder 6 KG| 3dimensionals (accessed Nov. 23, 2023)[Online]. Available: <https://www.3dimensionals.de/formlabs-nylon-12-sls-powder-2443#attr=5152,5148,5149,5150,5151,21939,25482> .
5. de Sousa Alves BA, Kontziampasis D, Soliman AH. The quest for the holy grail of 3D printing: A critical review of recycling in polymer powder bed fusion additive manufacturing. *Polymers* 2024;16(16):2306. doi: 10.3390/POLYM16162306.
6. Ligon SC, Liska R, Stampfl J, et al. Polymers for 3D Printing and customized additive manufacturing. *Chem Rev* 2017;117(15):10212 – 10290. doi: 10.1021/acs.chemrev.7b00074.
7. Feng L, Wang Y, Wei Q. PA12 powder recycled from SLS for FDM. *Polymers (Basel)* 2019;11(4):727. doi: 10.3390/polym11040727.
8. Wang L, Kiziltas A, Mielewski DF, et al. Closed-loop recycling of polyamide12 powder from selective laser sintering into sustainable composites. *J Clean Prod* 2018;195:765-772. doi: 10.1016/j.jclepro.2018.05.235.
9. Paolucci F, van Mook MJH, Govaert LE, et al. Influence of post-condensation on the crystallization kinetics of PA12: From virgin to reused powder. *Polymer (Guildf)* 2019;175:161-170. doi: 10.1016/j.polymer.2019.05.009.
10. US11046004B2 - Apparatus for treatment of residual thermoplastic powder - Google Patents (accessed Nov. 23, 2023)[Online]. Available: <https://patents.google.com/patent/US11046004B2/en> .
11. Dotchev K, Yusoff W. Recycling of polyamide 12 based powders in the laser sintering process. *Rapid Prototyp J* 2009;15(3):192-230. doi: 10.1108/13552540910960299.

12. Wegner A, Mielicki C, Grimm T, et al. Determination of robust material qualities and processing conditions for laser sintering of polyamide 12. *Polym Eng Sci* 2014;54(7):1540-1554. doi: 10.1002/pen.23696.
13. Arai S, Tsunoda S, Kawamura R, et al. Comparison of crystallization characteristics and mechanical properties of poly(butylene terephthalate) processed by laser sintering and injection molding. *Mater Des* 2017;113: 214-222. doi: 10.1016/j.matdes.2016.10.028.
14. Wudy K, Drummer D. Aging effects of polyamide 12 in selective laser sintering: Molecular weight distribution and thermal properties. *Addit Manuf* 2019;25:1-9. doi: 10.1016/j.addma.2018.11.007.
15. Wudy K, Drummer D. Aging behavior of polyamide 12: Interrelation between bulk characteristics and part properties. In: *Solid Freeform Fabrication 2016: Proceedings of the 27th Annual International Solid Freeform Fabrication Symposium - An Additive Manufacturing Conference, SFF 2016*, 2016.
16. Goodridge RD, Hague RJM, Tuck CJ. Effect of long-term ageing on the tensile properties of a polyamide 12 laser sintering material. *Polym Test* 2010;29(4):483-494. doi: 10.1016/j.polymertesting.2010.02.009.
17. Wudy K, Drummer D, Kühnlein F, Drexler M. Influence of degradation behavior of polyamide 12 powders in laser sintering process on produced parts. In: *AIP Conference Proceedings*, 2014. doi: 10.1063/1.4873873.
18. Weinmann S, Bonten C. Recycling of PA12 powder for selective laser sintering. In: *AIP Conference Proceedings*. American Institute of Physics Inc., Nov. 2020. doi: 10.1063/5.0029945.
19. Dimensions for specimen 1A of ISO 527-2-1996 standard | Download Scientific Diagram (accessed Oct. 30, 2023)[Online]. Available: https://www.researchgate.net/figure/Dimensions-for-specimen-1A-of-ISO-527-2-1996-standard-for-the-determination-of-tensile_fig3_335005103 .
20. Jevtić I, et al. Printing orientation influence on tensile strength of PA12 specimens obtained by SLS. *J Mech Sci Technol* 2023;37(11):5549-5554. doi: 10.1007/S12206-023-2306-4/METRICS.
21. Fuse 1+ 30W: Ein kompakter SLS-3D-Drucker (selektives Lasersintern) | Formlabs(accessed Oct. 30, 2023) [Online]. Available: <https://formlabs.com/de/3d-printers/fuse-1/> .
22. Calignano F, Giuffrida F, Galati M. Effect of the build orientation on the mechanical performance of polymeric parts produced by multi jet fusion and selective laser sintering. *J Manuf Process* 2021;65:271-282. doi: 10.1016/J.JMAPRO.2021.03.018.

Graphical Abstract



Declaration of interests

☐ The authors declare that they have no known competing financial interests or personal relationships that could have appeared to influence the work reported in this paper.

☒ The authors declare the following financial interests/personal relationships which may be considered as potential competing interests:

Conflict statement: Bruno Alexander de Sousa Alves reports a relationship with Ford Motor Company Ltd that includes: employment and non-financial support. The authors declare that they have no known competing financial interests or personal relationships that could have appeared to influence the work reported in this paper.